

***In vivo* real-time recording of UV-induced changes in the autofluorescence of a melanin-containing fungus using a micro-spectrofluorimeter and a low-cost webcam**

V. Raimondi^{1*}, G. Agati¹, G. Cecchi¹, I. Gomoiu², D. Lognoli¹, and L. Palombi¹

¹*Nello Carrara' Applied Physics Institute - National Research Council, Via Madonna del Piano 10, I- 50019 Sesto Fiorentino, Firenze, Italy*

²*National Arts University of Bucharest, Institute of Biology, Splaiul Independentei, 296, R-77700 Bucharest, Romania*
*v.raimondi@ifac.cnr.it

Abstract: An optical epifluorescence microscope, coupled to a CCD camera, a standard webcam and a microspectrofluorimeter, are used to record *in vivo* real-time changes in the autofluorescence of spores and hyphae in *Aspergillus niger*, a fungus containing melanin, while exposed to UV irradiation. The results point out major changes in both signal intensity and the spectral shape of the autofluorescence signal after only few minutes of exposure, and can contribute to the interpretation of data obtained with other fluorescence techniques, including those, such as GPF labeling, in which endogenous fluorophores constitute a major disturbance.

©2009 Optical Society of America

OCIS codes: (300.6280) Spectroscopy, fluorescence and luminescence; (170.1420) Biology; (170.6280) Spectroscopy, fluorescence and luminescence; (180.2520) Fluorescence microscopy; (170.3880) Medical and biological imaging.

References and links

1. G. Palumbo, and R. Pratesi, *Laser and current optical techniques in biology* (ESP RSC Publishing, Cambridge, 2004).
2. N. Billinton, and A. W. Knight, "Seeing the wood through the trees: a review of techniques for distinguishing green fluorescent protein from endogenous autofluorescence," *Anal. Biochem.* **291**(2), 175–197 (2001).
3. J. K. Li, E. C. Asali, A. E. Humphrey, and J. J. Horvath, "Monitoring cell concentration and activity by multiple excitation fluorometry," *Biotechnol. Prog.* **7**(1), 21–27 (1991).
4. S. Marose, C. Lindemann, and T. Scheper, "Two-dimensional fluorescence spectroscopy: a new tool for on-line bioprocess monitoring," *Biotechnol. Prog.* **14**(1), 63–74 (1998).
5. M. Ganzlin, S. Marose, X. Lu, B. Hitzmann, T. Scheper, and U. Rinas, "In situ multi-wavelength fluorescence spectroscopy as effective tool to simultaneously monitor spore germination, metabolic activity and quantitative protein production in recombinant *Aspergillus niger* fed-batch cultures," *J. Biotechnol.* **132**(4), 461–468 (2007).
6. A. R. Graham, "Fungal autofluorescence with ultraviolet illumination," *Am. J. Clin. Pathol.* **79**(2), 231–234 (1983).
7. M. Dellinger, M. Geze, R. Santus, E. Kohen, C. Kohen, J. G. Hirschberg, and M. Monti, "Imaging of cells by autofluorescence: a new tool in the probing of biopharmaceutical effects at the intracellular level," *Biotechnol. Appl. Biochem.* **28**(Pt 1), 25–32 (1998).
8. P. Asawanonda, and C. R. Taylor, "Wood's light in dermatology," *Review International Journal of Dermatology* **38**(11), 801–807 (1999).
9. D. M. Elston, "Fluorescence of fungi in superficial and deep fungal infections," *BMC Microbiol.* **1**(1), 21 (2001).
10. G. Méjean, J. Kasparian, J. Yu, S. Frey, E. Salmon, and J. P. Wolf, "Remote detection and identification of biological aerosols using a femtosecond terawatt lidar system," *Appl. Phys. B* **78**, 535–537 (2004).
11. V. Sivaprakasam, A. L. Huston, C. Scotto, and J. D. Eversole, "Multiple UV wavelength excitation and fluorescence of bioaerosols," *Opt. Express* **12**(19), 4457–4466 (2004).
12. K. Davitt, Y.-K. Song, W. R. Patterson III, A. V. Nurmikko, M. Gherasimova, J. Han, Y.-L. Pan, and R. K. Chang, "290 and 340 nm UV LED arrays for fluorescence detection from single airborne particles," *Opt. Express* **13**(23), 9548–9555 (2005).
13. H. Kanaani, M. Hargreaves, Z. Ristovski, and L. Morawska, "Performance assessment of UVAPS: influence of fungal spore age and air exposure," *J. Aerosol Sci.* **38**(1), 83–96 (2007).
14. C. Arcangeli, L. Zucconi, S. Onofri, and S. Cannistraro, "Fluorescence study on whole Antarctic fungal spores under enhanced UV irradiation," *J. Photochem. Photobiol. B* **39**(3), 258–264 (1997).

15. C. Arcangeli, W. Yu, S. Cannistraro, and E. Gratton, "Two-photon autofluorescence microscopy and spectroscopy of Antarctic fungus: new approach for studying effects of UV-B irradiation," *Biopolymers* **57**(4), 218–225 (2000).
16. D. Rativa, J. P. Batista Barbalho, J. Ferreira Martins Filho, R. Evangelista de Araujo, A. Stevens, L. Gomes, L. Gonzaga de Castro Souza Filho, and A. Marsden, "Perspectives on in vitro fungal diagnosis with UV light," *Revista Brasileira de Engenharia Biomédica* **23**, 25–30 (2007).
17. M. Bengtsson, S. Wallström, M. Sjöholm, R. Grönlund, B. Anderson, A. Larsson, S. Karlsson, S. Kröll, and S. Svanberg, "Fungus covered insulator materials studied with laser-induced fluorescence and principal component analysis," *Appl. Spectrosc.* **59**(8), 1037–1041 (2005).
18. M. Bengtsson, R. Grönlund, M. Sjöholm, C. Abrahamsson, A. D. Demfalk, S. Wallström, A. Larsson, P. Weibring, S. Karlsson, S. M. Gubanski, S. Kröll, and S. Svanberg, "Fluorescence lidar imaging of fungal growth on high-voltage outdoor composite insulators," *Opt. Lasers Eng.* **43**(6), 624–632 (2005).
19. V. Raimondi, L. Palombi, G. Cecchi, D. Lognoli, M. Trambusti, and I. Gomoiu, "Remote detection of laser-induced autofluorescence on pure cultures of fungal and bacterial strains and their analysis with multivariate techniques," *Opt. Commun.* **273**(1), 219–225 (2007).
20. L. Rigacci, R. Alterini, P. A. Bernabei, P. R. Ferrini, G. Agati, F. Fusi, and M. Monici, "Multispectral imaging autofluorescence microscopy for the analysis of lymph-node tissues," *Photochem. Photobiol.* **71**(6), 737–742 (2000).
21. F. Sidney, Velick, "Spectra and structure in enzyme complexes of pyridine and flavine nucleotides," in *Light and Life*, W. D. McElroy and B. Glass, eds. (Johns Hopkins Press, Baltimore, 1961).
22. K. König, M. W. Berns, and B. J. Tromberg, "Time-resolved and steady-state fluorescence measurements of beta-nicotinamide adenine dinucleotide-alcohol dehydrogenase complex during UVA exposure," *J. Photochem. Photobiol. B* **37**(1-2), 91–95 (1997).
23. J. Eng, R. M. Lynch, and R. S. Balaban, "Nicotinamide adenine dinucleotide fluorescence spectroscopy and imaging of isolated cardiac myocytes," *Biophys. J.* **55**(4), 621–630 (1989).
24. F. Joubert, H. M. Fales, H. Wen, C. A. Combs, and R. S. Balaban, "NADH enzyme-dependent fluorescence recovery after photobleaching: applications to enzyme and mitochondrial reactions kinetics, in vitro," *Biophys. J.* **86**(1), 629–645 (2004).
25. L. M. Tiede, M. G. Nichols; LeA, "Photobleaching of reduced nicotinamide adenine dinucleotide and the development of highly fluorescent lesions in rat basophilic leukemia cells during multiphoton microscopy," *Photochem. Photobiol.* **82**(3), 656–664 (2006).
26. K. König, T. Krasieva, E. Bauer, U. Fiedler, M. W. Berns, B. J. Tromberg, and K. O. Greulich, "Cell damage by UVA radiation of a mercury microscopy lamp probed by autofluorescence modifications, cloning assay and comet assay," *J. Biochem. Opt.* **1**, 217–222 (1996).
27. C. A. Combs, and R. S. Balaban, "Direct imaging of dehydrogenase activity within living cells using enzyme-dependent fluorescence recovery after photobleaching (ED-FRAP)," *Biophys. J.* **80**(4), 2018–2028 (2001).
28. P. Kayatz, G. Thumann, T. T. Luther, J. F. Jordan, K. U. Bartz-Schmidt, P. J. Esser, and U. Schraermeyer, "Oxidation causes melanin fluorescence," *Invest. Ophthalmol. Vis. Sci.* **42**(1), 241–246 (2001).
29. R. C. Benson, R. A. Meyer, M. E. Zaruba, and G. M. McKhann, "Cellular autofluorescence—is it due to flavins?" *J. Histochem. Cytochem.* **27**(1), 44–48 (1979).
30. I. Gomoiu, E. Saratopoulou, Z. Kollia, A. C. Cefalas, J. van Loon, D. Mogaldea, D. Hasegan, and V. Valeanu, "Colored fungal spores as candidates for space experiments," *Orig. Life Evol. Biosph.* (to be published).

1. Introduction

Fluorescence-based techniques are widely applied in investigating biological samples [1], with a considerable increase in recent years in the use of fluorescence microscope techniques based on labeling with Green Fluorescent Protein (GFP) or with other fluorophores [2]. In particular, fungi have been studied via several fluorescence-based techniques for applications in various fields, from bioprocess monitoring [3–5] and health-related applications [6–9] to the environment, defense, and public security [10–13].

Few studies, however, have investigated the spectral features of endogenous fluorescence, or autofluorescence, of fungal species. 2-D fluorescence spectra at low spectral resolution (20 nm) are reported in [4,5], where the endogenous fluorescence of the coenzyme NAD(P)H and of aminoacids is identified with 2-D fluorescence spectroscopy on fed-batch cultures of *Aspergillus niger*. In these studies, fluorescence is used to monitor metabolic activity during a bioprocess with GFP labeling. An additional unidentified fluorophore emitting between 490 and 540 nm, which was interpreted as a flavoprotein, is regarded as an indicator of fungal metabolic activity [5]. High spectral resolution fluorescence of a UV-irradiated Antarctic fungus was investigated both with a spectrofluorimeter on suspensions of fungal spores [14] and with two-photon fluorescence microscopy and spectroscopy [15]. More recently, Laser Induced Fluorescence (LIF) spectra were studied on pure cultures of fungal strains both in the laboratory [16,17] and in a standoff configuration for different remote sensing applications

[18,19]. Nevertheless, there is still a general lack of knowledge on the fluorescence spectral features of fungi, their origin, and how they are modified during UV irradiation.

This paper focuses on the synergetic use of a microscope-coupled spectrofluorimeter, a webcam, and a CCD camera for the detection of the autofluorescence features of fungi and their *in vivo*, real-time modifications at microscopic level. Here the technique is applied to a melanin-containing filamentous fungus, *Aspergillus niger*, while it is irradiated at 365 nm with the microscope lamp. The objective was to obtain an insight into the origin of the fluorescence spectral features and to contribute to the interpretation of data obtained using other fluorescence-based techniques, such as two-dimensional fluorescence spectroscopy for bioprocess monitoring, fluorescence microscopy, LIF technique, etc., and including those techniques where endogenous fluorophores constitute a major disturbance. In addition, this study can be exploited to gain further knowledge on the effects of UV irradiation on fungi and thus to contribute to various studies in which fungi are used as bioindicators, which range from environmental to space applications.

2. Experimental

The measurements were conducted on a melanin-containing fungal strain (*Aspergillus niger*) and were carried out using an inverted epifluorescence microscope equipped with a CCD camera and interferential filters. The microscope was also fiber-coupled to a spectrometer, to obtain spectrally-resolved fluorescence signals that would refer to single microstructures of the sample. A webcam was also used to record real-time changes in the fluorescence of the fungus. The following subsections provide a short description of the strain examined, how we prepared the samples, and which instrumentation we used for this study.

2.1 Materials and methods

Aspergillus niger is a filamentous fungus that can be isolated from soil, plant debris, and also from indoor air environment. Figure 1 shows a Petri dish with an *Aspergillus niger* colony and its outward morphology.

Colonies on nutrient medium (potato-dextrose-agar) have a rapid growth (10 mm/day), with abundant submerged mycelium and few aerial hyphae. The latter can be more or less yellow colored, whereas those hyphae in the reverse of the colony, that is submerged hyphae, are usually white. Conidiophores grow up vertically, that is in a perpendicular direction with respect to the mother hyphae which lays on the surface of nutrient medium. They are smooth, septate or nonseptate, and brown; their length and diameter varies between 200 μm and 400 μm and 7 μm and 10 μm , respectively. Conidial heads are radiate, become loosely columnar at maturity, and are blackish-brown or black with globose vesicles (50-100 μm in diameter) covered by two series of phialides. Conidia form chains on the phialides.



Fig. 1. Photo of the fungal strain (*Aspergillus niger*) isolated and cultivated in the laboratory. The dark brownish color of the colony is due to the melanin high content of this species.

They are globose and vary in diameter between 2.5 μm and 4.2 μm . Initially, they are smooth, but later become spinulose and black because of their melanin content.

The fungal strain that we examined was isolated from frescoes of the Ovidenia Church, in Bistrita area in Romania. We prepared the samples as follows: the collected sample - taken under sterile conditions - was vigorously agitated in 10 min vortexing and then diluted it (1/10). Duplicate and triplicate 1 ml volumes of appropriate dilutions were inoculated onto DPA (dextrose-potato-agar) as nutrient medium, and after 6 days of incubation at 28°C we

isolated pure cultures. The fungus was identified according to its cultural characteristics and to the morphology of its hyphae and spores.

We prepared the slides for microscopic observation using spores and hyphae from 13-day-old and 21-day-old cultures grown on potato-glucose-agar (Fluka) plates. For each type of culture, we prepared the slides in two different ways: in the first case (dry sample), we placed a drop of distilled water on the slide and added some material scratched from the culture with a loop so as to obtain a suspension of the fungal spores and hyphae; we then waited until the water evaporated completely. In the second case (wet sample), we added a drop of distilled water to a slide already prepared as described above. The slides were examined at the microscope immediately after their preparation.

2.2 Instrumentation

The measurements were carried out using an inverted epifluorescence microscope (Diaphot, Nikon) coupled to a CCD camera, a multichannel spectral analyzer (microspectrofluorimeter) and an eyepiece-mounted webcam.

A technical drawing of the experimental set-up is sketched in Fig. 2.

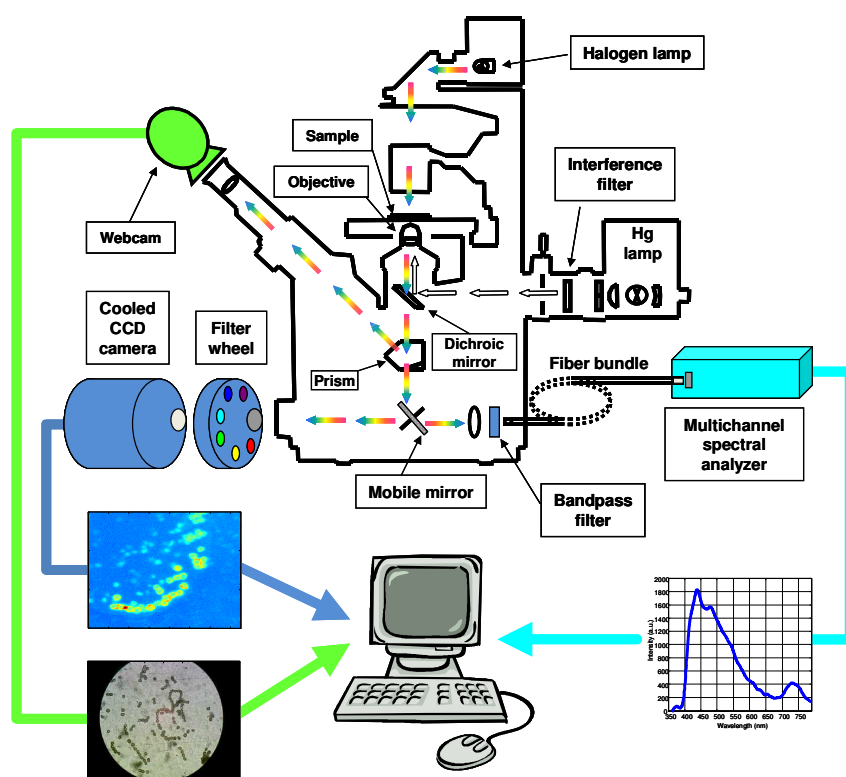


Fig. 2. Technical drawing depicting the experimental set-up used for the autofluorescence measurements. The set-up integrated an epifluorescence microscope with a CCD camera, a multichannel spectral analyzer (microspectrofluorimeter) and an eyepiece-mounted webcam.

The epifluorescence microscope (Diaphot, Nikon) was equipped with a high-pressure mercury lamp (HBO 100 W, Osram) as a light source. The fluorescence excitation at 365 nm was selected out of the collimated Hg-lamp light using a 10-nm bandwidth interference filter (365FS10-25, Andover Corporation). A 45 degrees dichroic mirror (ND400, Nikon) folded the excitation radiation through the objective ($\times 10$ or an oil-immersion $\times 100$ Fluor (NA = 1.3) objective) of the microscope focalizing it on the sample. The mean power at the sample was about 0.3 W/cm^2 with a $\times 100$ objective. Backscattered and fluorescence radiation was collected by the same objective. The collected fluorescence radiation above 400 nm passed

through the dichroic mirror and then was deflected by a prism and a mobile mirror towards either the microscope eyepieces (coupled to a webcam) or a CCD camera or a spectral analyzer. The microscope was also equipped with a white light (halogen lamp) source to acquire transmission images. The halogen lamp radiation transmitted by the sample was collected by the microscope objective. The transmitted radiation above 400 nm passed through the dichroic mirror and was deflected towards either the microscope eyepiece (coupled to a webcam) or the CCD camera.

The CCD camera was a high-sensitivity cooled CCD camera (Chroma CX260E, DTA s.r.l.) featuring a 512×512 pixel detector (KAF261E, Kodak). Images were digitized with a 14 bit (16384 gray levels) dynamics. A motorized filter wheel, positioned in front of the CCD detector, hosted 8 different interference filters that could be used for multi-spectral sequential imaging. For these measurements, we used two 40-nm bandwidth interference filters centered at 450 and 550 nm, respectively (450FS40-25 and 550FS40-25, Andover Corporation). Integration time varied up to 30 s, depending on the signal intensity. The image spatial calibration with the CCD camera, when using the $\times 10$ Plan Fluor Nikon objective, was $0.79 \mu\text{m pixel}^{-1}$. We also used a standard webcam, that was coupled to the microscope eyepiece, for a quick, real-time record of changes in the fungal autofluorescence, although the optical quality was poorer.

Microfluorescence spectra were recorded with a CCD multichannel spectral analyzer (PMA 11-C5966, Hamamatsu), coupled to the microscope through an optical fiber bundle (1-mm diameter). Residual excitation light was removed with a long-pass filter (GG400, Schott Glas). Further detail on the microspectrofluorimeter is given in [20]. The spectra were acquired in the 300–800 nm spectral range with an integration time of 10 s. The actual area measured by the microspectrofluorimeter on the sample was a $10\text{-}\mu$ diameter spot when using the $\times 100$ objective. All fluorescence spectra were corrected for the spectral response of the optical system by using the correction spectral curve obtained from the comparison between the reference spectrum and the observed spectrum of a calibration white lamp.

3. Results

In general, the samples examined contained mainly spores that showed a faint to very-faint blue fluorescence when observed under UV illumination.

Figure 3 shows the transmission images, the fluorescence images, and the fluorescence spectra acquired on spores of two samples using the $\times 100$ objective: Fig. 3(a), Fig. 3(b) and Fig. 3(c) refer to a sample prepared from a 13-day-old culture and Fig. 3(d), Fig. 3(e) and Fig. 3(f) refer to a sample prepared from a 21-day-old culture. The spectra in Fig. 3(c) and Fig. 3(f) show a fluorescence band in the blue with at least two main contributions: at about 440 nm and at 490 nm (the peak at 730 nm is due to the second order of the residual UV excitation). The younger culture [Fig. 3(b)] shows a more intense fluorescence with respect to the older one [Fig. 3(e)] and has its emission maximum at about 440 nm. The fluorescence of the samples prepared from the older culture was lower, and only a very faint blue fluorescence was visible in the fluorescence image [Fig. 3(d)].

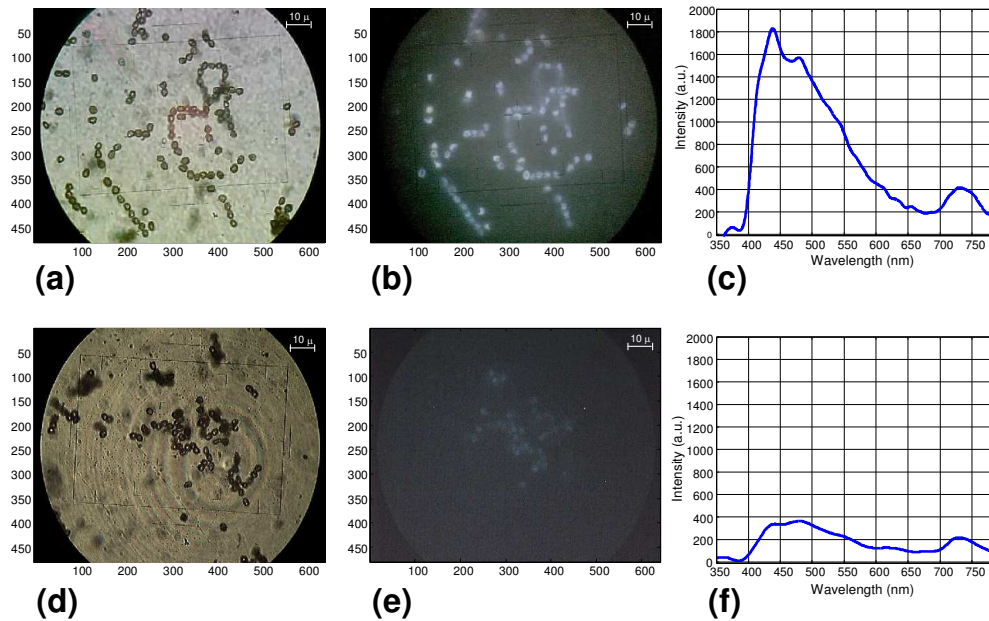


Fig. 3. Transmission images, fluorescence images and fluorescence spectra of isolated spores of *Aspergillus niger*: (a), (b), and (c) were acquired on a dry sample prepared from a 13-day-old culture. (d), (e), and (f) were acquired on a dry sample prepared from a 21-day-old culture. All data were acquired using the x100 objective. Images were acquired using the webcam; fluorescence spectra were acquired using the microspectrofluorimeter.

Figure 4 shows the changes in endogenous fluorescence of a group of spores while exposed for about 30 min to UV at 365 nm of the microscope lamp. Figure 4(a) shows the temporal sequence of fluorescence spectra acquired with the microspectrofluorimeter on the spores during UV exposure, while Fig. 4(b) shows the sequence of fluorescence images acquired using the webcam on the same sample. Fluorescence spectra acquired at the beginning of the sequence, after 6.4 min, and at the end of the sequence, are reported in Fig. 4(c). The spores show a blue fluorescence with main contributions at about 440 nm and at about 480 nm. Further contributions at 540 nm and 610 nm were also present. In the beginning, the spores showed a very faint blue fluorescence, with an emission maximum at about 480 nm. This blue fluorescence decreased very quickly as soon as the sample was exposed to the UV, as is evident from Fig. 4(c). After about 20 min of continuous UV exposure, however, the spores began to fluoresce again, but in a different spectral region [Fig. 4(d)]. This was apparent both from the fluorescence spectra and from the fluorescence images in which an increasing yellowish fluorescence was recorded. This fluorescence became very strong after about half an hour of continuous UV exposure and featured a maximum at about 540 nm [Fig. 4(c) and Fig. 4(d)].

Figure 5 shows some close-ups of the transmission and fluorescence images acquired using the webcam and referring to the same temporal sequence of Fig. 4. The comparison between the transmission image before [Fig. 5(a)] and after [Fig. 5(b)] UV exposure points out a discoloration of the only spores exposed to UV, as can be inferred from the picture in Fig. 5(c), where the UV-induced fluorescence is superimposed on the transmission image [note that this image has shifted slightly as compared with the previous ones]. In fact, all spores in Fig. 5(a) are initially brownish, while in Fig. 5(b) only the spores exposed to UV irradiation (red circled in Fig. 5(b)) became whitish at the end of the sequence. The area illuminated by the UV lamp corresponds, in fact, to the circle inscribed in the main rectangle of the microscope crosshair, as it can be observed in Fig. 5(c), where the UV-induced fluorescence image is superimposed on the transmission image, and in and in [Media 1](#) of Fig. 6(a).

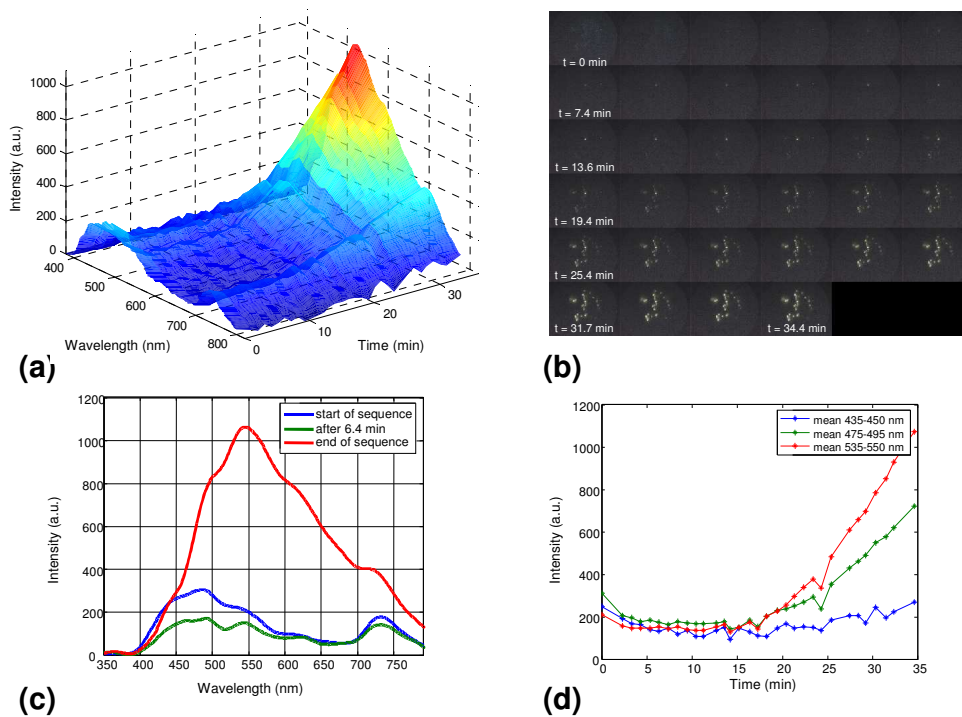


Fig. 4. Temporal sequence of endogenous fluorescence spectra and images of fungal spores (21-day old culture; dry sample). All data were acquired using the x100 objective. Images were acquired using the webcam; fluorescence spectra were acquired using the microspectrofluorimeter. (a) Sequence of fluorescence spectra. (b) Sequence of fluorescence images acquired using the webcam (time step: about 1 min). (c) Fluorescence spectra acquired at three selected times during the sequence: start of the sequence ($t = 0$ min), after a few minutes of exposure ($t = 6.4$ min), and at the end of the sequence ($t = 34.6$ min). (d) Trend of the main fluorescence contributions as a function of time.

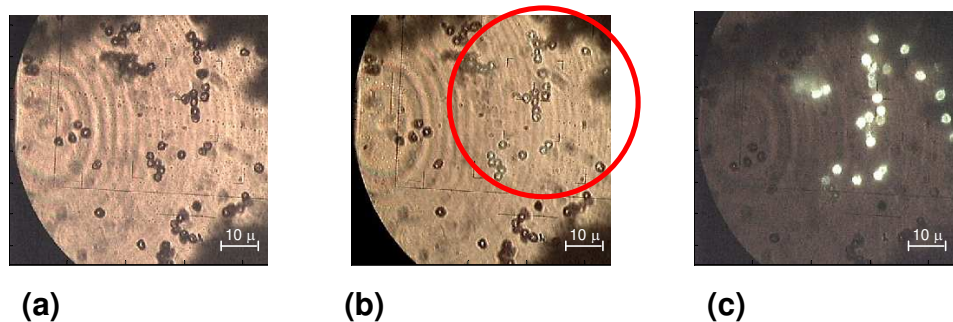


Fig. 5. Close-ups of transmission and fluorescence images, acquired using the webcam, referring to fluorescence data in Fig. 4. (a) Transmission image before UV exposure. (b) Transmission image at the end of the temporal sequence (35-min long UV exposure). The red circle indicates the area irradiated by the UV light. (c) Fluorescence image superimposed on the transmission image. The fluorescing spores indicate the area irradiated by the UV light.

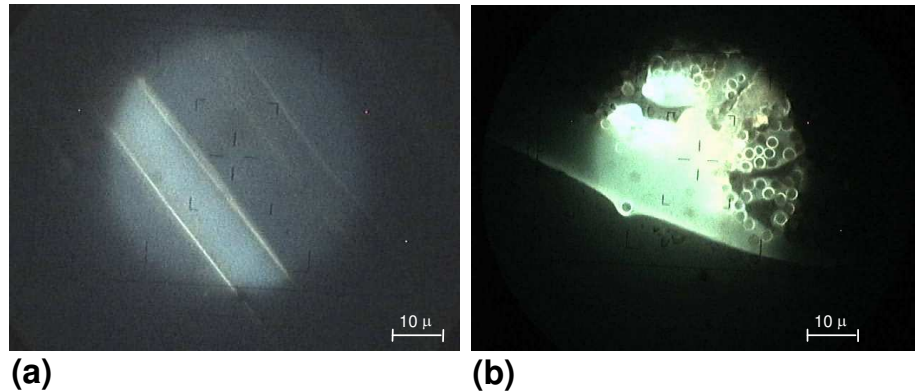


Fig. 6. *In vivo* real-time recording of endogenous fluorescence modifications due to UV irradiation using the webcam on: (a) hypha ([Media 1](#)), and (b) spores ([Media 2](#)) of *Aspergillus niger* (21-day-old culture; wet sample). The images were acquired using the x100 objective.

In vivo real time recording of the UV-induced changes in the fluorescence of hyphae and spores are shown in Fig. 6. Figure 6(a) reports the changes of the fluorescence of an hypha induced by the exposition to the UV: the hypha initially featured a blue fluorescence, but rapidly shows an increasing yellow fluorescence, which clearly originated from its walls. The recording also shows some isolated spores that became strongly yellow fluorescent as they were exposed to UV, although the origin of the yellow fluorescence of the spores is not clear in this record due to the fact that only the hypha is focused. In the upper right of the image there is also another hypha (out of focus), as it can be easily inferred from the transmission image at the end of the recording [[Media 1](#) in Fig. 6(a)]. Figure 6(b) shows the recording of the fluorescence changes due to UV exposition on a group of spores of the same sample. In this case, the spores in the focal plane clearly showed how the strong yellow fluorescence came from the spore walls.

Figure 7 shows a sequence of fluorescence spectra acquired using the micro-spectrofluorimeter [Fig. 7(a)] and fluorescence images acquired using the webcam [Fig. 7(b)] taken on a sample of spores to which a drop of distilled water was added (wet sample). The addition of water had the effect of reducing considerably the time required for the insurgence of the strong yellow fluorescence at 540 nm. The spores emitted strong yellow fluorescence only a few minutes after exposure to the UV, while the dry sample required about 20 min of continuous UV exposure. Fluorescence spectra acquired at the beginning of the sequence, after 4.3 min, and at the end of the sequence are reported in Fig. 7(c). Also in this case, the spores initially showed a faint blue fluorescence, with main contributions at about 440 nm and at about 480 nm, and further contributions at 540 nm and 610 nm. Also in this case (wet sample), the emission maximum was at 480 nm, and there were no significant shifts of the other contributions as compared with the dry sample [Fig. 4(c)]. Differently from the dry sample, however, after about 5 min the fluorescence started to decrease very quickly, and the main contribution to the fluorescence spectrum again was in the blue region [Fig. 7(d)].

Another effect of UV exposure on the wet sample is shown in Fig. 8. The transmission images taken before and after the exposure to UV, shown respectively in Fig. 8(a) and Fig. 8(b), make it clear that there is a discoloration of the spores due to the UV. In addition, the fluorescence image [Fig. 8(c)] acquired about 5 min after exposure to UV, i.e. when the yellow fluorescence reached its maximum emission [Fig. 7(d)], shows that the fluorophores responsible for the yellow fluorescence were mainly located in the spore walls. After about 15 min, the spores again emitted a predominantly blue fluorescence [Fig. 8(d)], which was uniformly distributed inside the spores and has the same spectral shape as the initial blue fluorescence observed at the beginning of the UV exposure, but slightly more intense, as shown in Fig. 7(b).

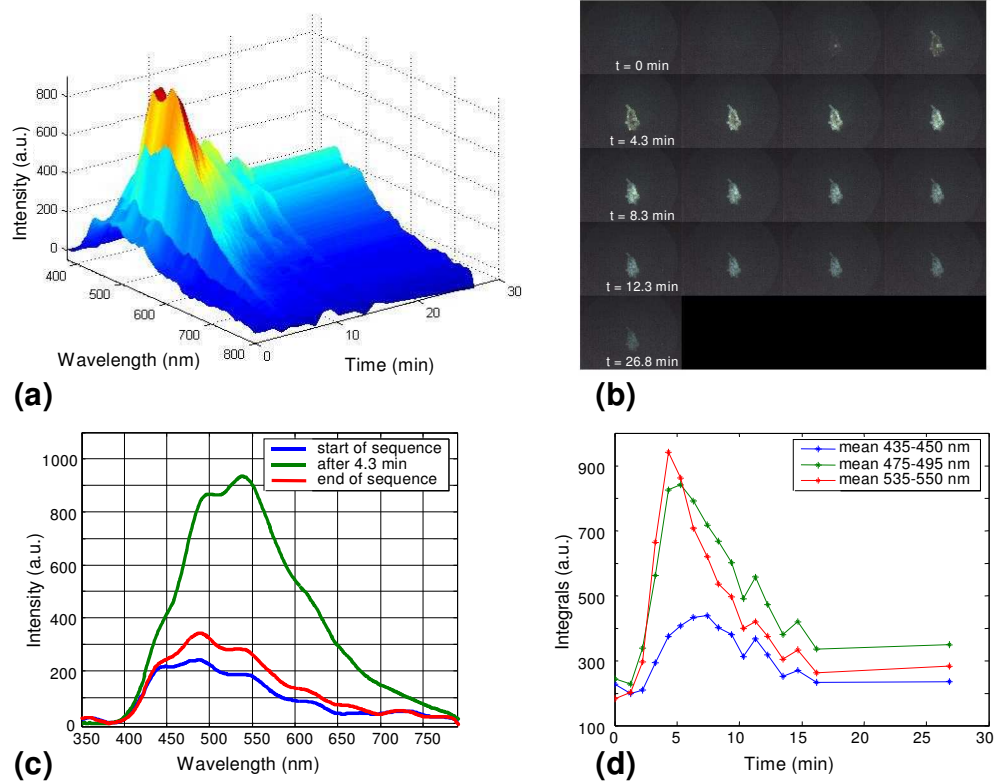


Fig. 7. Temporal sequence of endogenous fluorescence spectra and images of fungal spores (21-day-old culture; wet sample). All data were acquired using the x100 objective. Images were acquired using the webcam; fluorescence spectra were acquired with the microspectrofluorimeter. (a) Sequence of fluorescence spectra; (b) sequence of fluorescence images acquired using the webcam (time step: about 1 min). (c) three fluorescence spectra acquired at the three selected times during the sequence: t_0 (start of the sequence), $t_0 + 4.3$ min (maximum emission of yellow fluorescence), $t_0 + 26.8$ min (end of the sequence); (d) trend of the main fluorescence contributions as a function of time.

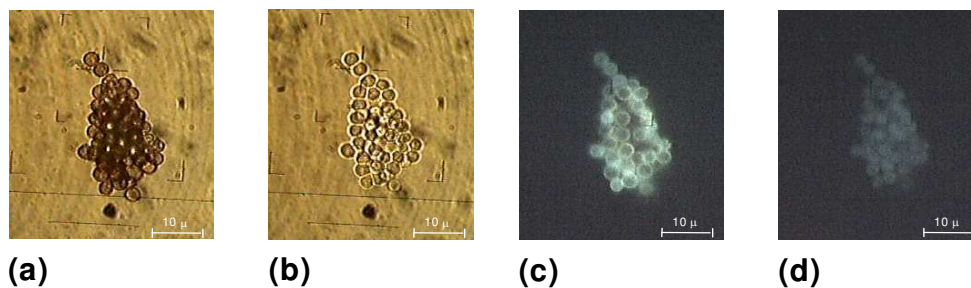


Fig. 8. Close-ups of transmission and fluorescence images, acquired using the webcam, referring to fluorescence data shown in Fig. 7. (a) Transmission image before UV exposure; (b) Transmission image at the end of the sequence (26.8-min long UV exposure). (c) Fluorescence image at $t_0 + 4.3$ min (maximum emission of yellow fluorescence). (d) Fluorescence image at the end of the sequence (26.8-min long UV exposure).

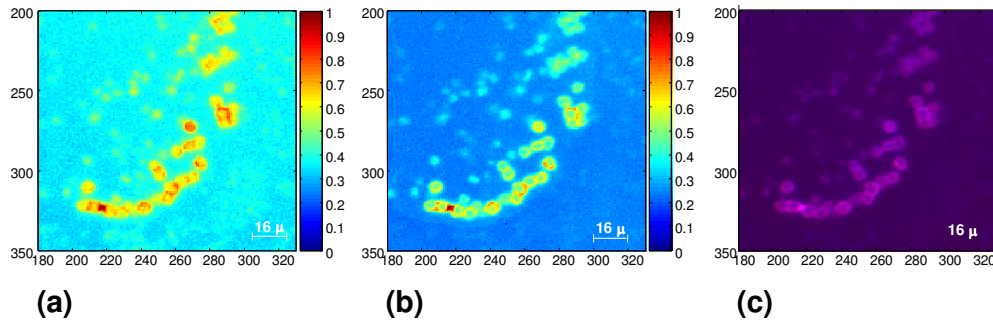


Fig. 9. False-color coded fluorescence images of spores (13-day-old culture; dry sample) acquired using the CCD camera and interferential filters. The images were acquired with the x10 objective. Excitation is at 365 nm. Images are normalized to the maximum intensity. (a) Fluorescence emitted at 450 nm. (b) Fluorescence emitted at 550 nm. (c) RB merging of the two fluorescence images (450-nm fluorescence on the blue (B) channel and 550-nm fluorescence on the red (R) channel).

Fluorescence images were also acquired on a group of spores using the CCD camera equipped with interferential filters. Figure 9(a) shows a false-color coded fluorescence image acquired with the 450-nm interferential filter on a group of spores (13-day-old culture; dry sample), whereas Fig. 9(b) shows a false-color coded image acquired on the same sample using the 550-nm interferential filter. Red-yellow pixels in Fig. 9(a) indicate a more intense fluorescence intensity at 450 nm; red-yellow pixels in Fig. 9(b) indicate a more intense fluorescence intensity at 550 nm. Due to the low fluorescence signal, the images were acquired using the x10 objective. Integration time was 30 s. Figure 9(a) shows how the blue fluorescence was quite uniformly distributed inside the cytoplasm, while the yellow fluorescence [Fig. 9(b)] was mainly located in correspondence with the spore walls. This is clear also from the RB merging of the two images shown in Fig. 9(c), where the 450-nm fluorescence is associated with the blue (B) channel and the 550-nm fluorescence is associated with the red (R) channel.

4. Discussion

All the samples examined under UV illumination initially showed a faint to very-faint blue fluorescence. This fluorescence can be ascribed to the reduced form of the nicotinamide-adenine dinucleotide (phosphate) (NAD(P)H), which is known to emit fluorescence in the blue spectral region with a maximum of between 440 nm and 465 nm, depending on the binding and the sample environment [21,22]. In particular, the band with its emission maximum at about 440 nm can be attributed to the protein-bound NAD(P)H [21–23]. A considerably higher intensity of this band in the 13-day old culture [Fig. 3(c) and Fig. 3(f)] is consistent with the fact that, in these cultures, the spores are still kept in long chains [Fig. 3(a) and Fig. 3(b)] and this is known to be due to a proteinaceous disk located between two adjacent spores. On the contrary, most spores in the 21-day old culture are either spread as individuals or kept in very short chains [Fig. 3(d) and Fig. 3(e)], which leads to an overall lower content of proteins and thus of protein-bound NAD(P)H. This justifies a considerably higher fluorescence at 440 nm in the younger cultures due to an overall higher content of protein-bound NAD(P)H. Consistently, a higher fluorescence intensity in younger cultures was also observed in fungal bioaerosols with an UV aerodynamic particle sizer spectrometer, in which the percentage of fluorescent spores was found to decrease as they aged [13]. A greater fluorescence contribution at about 440 nm has already been observed also in viable cells [23]. Moreover, the fluorescence of viable myocytes showed a maximum at 447 nm, while nonviable myocytes were found to have a definitely lower fluorescence emission, with a consistent decrease in the contribution at 447 nm [23]. On the other hand, the decrease of this blue fluorescence immediately after exposition to UV [Fig. 4(c) and Fig. 4(d)] could be ascribed to a photobleaching effect and can be explained on the basis of the NADH photolysis

to NAD and reduced oxygen, proteins or other free-radical products [24,25]. A decrease in the NAD(P)H blue fluorescence due to photobleaching caused by UV exposure has already been observed in many other biological samples [22,26,27].

The emergence of a intense fluorescence band with a maximum at 540 nm after a longer exposition to the UV both in the dry and the wet samples [Fig. 4(a) and Fig. 4(c)] could instead involve the photo-oxidation of melanin, which is known to be present in this species abundantly. The oxidation of melanin and its strong yellow fluorescence have recently been observed in both retinal pigment epithelium and *in vitro*, where oxidized melanin was found to have an emission spectrum that peaked at 540 nm in the case of both synthetic melanin and isolated bovine melanosomes [28]. Further support to the interpretation of the strong yellow fluorescence as being due to the photo-oxidation of melanin is suggested by the fact that the fluorophore mainly responsible for the yellow fluorescence is located in the hyphae and cell walls [Fig. 6(a) and Fig. 6(b)]. This suggests that the fluorophore is a pigment, rather than flavins or flavoproteins, which also emit fluorescence typically between 530 and 560 nm [29], but are not confined to the cell walls. Similar results can also be observed in Fig. 8 and Fig. 9, where the blue fluorescence [Fig. 8(d) and Fig. 9(a)] is uniformly distributed inside the cytoplasm, as we could expect for NAD(P)H fluorescence, while the yellow fluorescence is mainly confined to the cell walls [Fig. 8(c) and Fig. 9(b)]. This again supports the hypothesis that the fluorophores causing yellow fluorescence were mainly located on the spore walls and were likely to be due to the melanin that is abundantly contained in this fungal species. A strong yellow fluorescence from the cell walls of a UV-stressed Antarctic fungus has also been observed using a two-photon fluorescence microscopy and was attributed to an unknown fluorophore, most probably a pigment [15]. The disappearance of the yellow fluorescence observed in the wet sample after a further UV exposure (Fig. 7) and the observation of a predominantly blue fluorescence, having the same spectral shape as the initial blue fluorescence observed at the beginning of the UV exposure, may be due to the photo-destruction of the melanin pigment which, being a photoprotector, initially prevents endogenous fluorophores from being effectively excited by UV. A photo-destruction process in the wet sample at the end of the 26.8-min long UV exposure is further supported by the discoloration of spores shown in Fig. 8(b). This type of discoloration has also been found in other studies devoted to investigating the effects of UVC irradiation on fungal spores to be used as bioindicators in space experiments [30]. After photo-oxidation of the melanin, due to continuous UV exposure, NAD(P)H fluorescence no longer shows such a rapid decrease, as we observed immediately after UV exposure in both the dry and the wet samples [Fig. 4(d) and Fig. 7(d)]. An explanation could be attributed to a different redox state of the cell, since the fractional contribution of the bound- and free NAD(P)H was then changed.

5. Conclusions

The use of a microspectrofluorimeter and a low-cost standard webcam, coupled to an inverted epifluorescence microscope, were used to investigate the features of endogenous fluorescence and the effects of the UV irradiation in a melanin-containing fungus. The use of a webcam made possible a quick acquisition of fluorescence images, even ones of very weak intensity, and contributed considerably to an interpretation of the full resolution fluorescence spectra acquired using the microspectrofluorimeter.

The use of this instrumentation on samples of *Aspergillus niger*, a weakly fluorescent fungus, made it possible to record in real-time the UV-induced effects in both spores and hyphae. Changes were observed in both the intensity and the spectral shape of the endogenous fluorescence after UV irradiation. Initially, an abrupt change occurred in the blue fluorescence intensity, interpreted as due to the photobleaching of NAD(P)H; however, after a few minutes of irradiation, a strong yellow fluorescence, which was attributed to the photo-oxidation of melanin, was observed at 540 nm. The effects of UV irradiation were considerably enhanced in the wet samples. Transmission images also showed a photobleaching effect on the irradiated spores. Further studies will address the effects of UV irradiation also in other fungal

strains in order to ascertain the role of pigments like melanin in the photo-oxidation of the samples.

Acknowledgments

This work was carried out within the framework of the cooperation agreement (Prot. N. 0002892, 18/12/2007) between the National Art University of Bucharest, Romania, and the CNR-IFAC, Italy. The authors also wish to acknowledge the contribution of the Romanian National Project 90-001 and the ICT-ONE Project, funded by the Regione Toscana, to carrying out this study.